Supporting information

Supplementary information for Dissolvable templates to prepare Pt-based porous metallic glass for oxygen reduction reaction

Xiong Liang[§a], Zehang Liu[a], Jianan Fu[b], Heting Zhang[a], Jinbiao Huang[a], Shuai Ren[a], Zhenxuan Zhang[a], Qing Chen[c], Yong Xiao[d],Wenqing Ruan*[a], Jiang Ma*[a]

[a]*Shenzhen Key Laboratory of High Perfrmance Nontraditional Manufacturing, College of Mechatronics and Control Engineering, Shenzhen University, Shenzhen, 518060, China.*

[b]*Department of Mechanics and Aerospace Engineering, Southern University of Science and Technology, Shenzhen, 518055, China.*

[c]*Department of Mechanical and Aerospace Engineering, The Hong Kong University of Science and Technology, Clear Water Bay, Kowloon, Hong Kong, China*

[d]*School of Materials Science and Engineering, Wuhan University of Technology*

[§]*These authors contributed equally to this work*

* To whom correspondence should be addressed: ruanwq@szu.edu.cn, majiang@szu.edu.cn

Content：

Supporting Notes1: Calculation of electron transfer number (n)

The electron transfer number (n) is calculated by the Koutecky-Levich equation at various electrode potentials.

$$\frac{1}{i} = \frac{1}{i_\kappa} + \frac{1}{i_d} = \frac{1}{nFA\kappa C_{O_2}} + \frac{1}{B\omega^{1/2}}$$

$$B = 0.2nFAC_{O_2}D_{O_2}^{2/3}V^{-1/6}$$

where i, i_κ and i_d represent measured, kinetic and diffusion-limiting current, respectively, n represents the transferred electron number per oxygen molecule. F is faraday constant (96485 C mol^{-1}). A is the geometric electrode area (0.196 cm^2); κ is the rate constant for ORR (m s^{-1}); C_{O2} is the saturated concentration of oxygen in 0.1 M KOH solution (1.2×10^{-6} mol cm^{-3}); D_{O2} is the diffusion coefficient of oxygen in 0.1 M KOH solution (1.9×10^{-5} cm^2 s^{-1}); V is the kinematic viscosity of solution (0.01 cm^2 s^{-1}); and ω is the angular rotation speed (rad s^{-1}). The constant 0.2 is adopted when the rotation speed is expressed in rpm.

Supplementary Note 2: Electrochemical characterization of the intrinsic activities of catalysts toward ORR

Electrochemical double-layer capacitance measurements were used to determine the electrochemically active surface areas (ECSA) of the electrocatalysts. The ECSA value was calculated based on the equation of ECSA = C_{dl}/C_S, where C_{dl} is the electrochemical double-layer capacitance and Cs is the specific capacitance. The Cs for a flat surface was generally found to be in the range of 20 to 60 μF cm^{-2} . In this work, we used a value of 20 μF cm^{-2}. For this, the potential window of cyclic voltammetric stripping was 1.07 V to 1.12 V versus RHE (0.1 M KOH solution). The scan rates were 3 mV s^{-1}, 5 mV s^{-1}, 10 mV s^{-1}, 20 mV s^{-1}, 40 mV s^{-1}, 50 mV s^{-1}, 60 mV s^{-1}, 80 mV $s^{-1}$and 100 mV s^{-1}. The C_{dl} was estimated by plotting the $\Delta j = (j_a - j_c)$ at 1.09 V (where j_c and j_a are the cathodic and anodic current densities, respectively) versus RHE against the scan rate, in which the slope was twice that of C_{dl}.

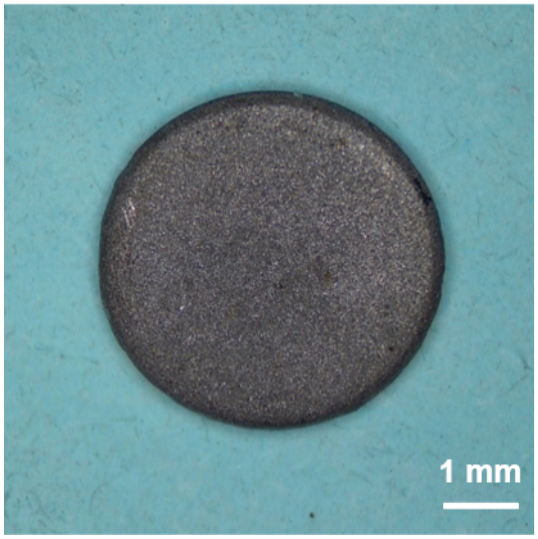

Fig. S1 The amorphous samples after hot pressing.

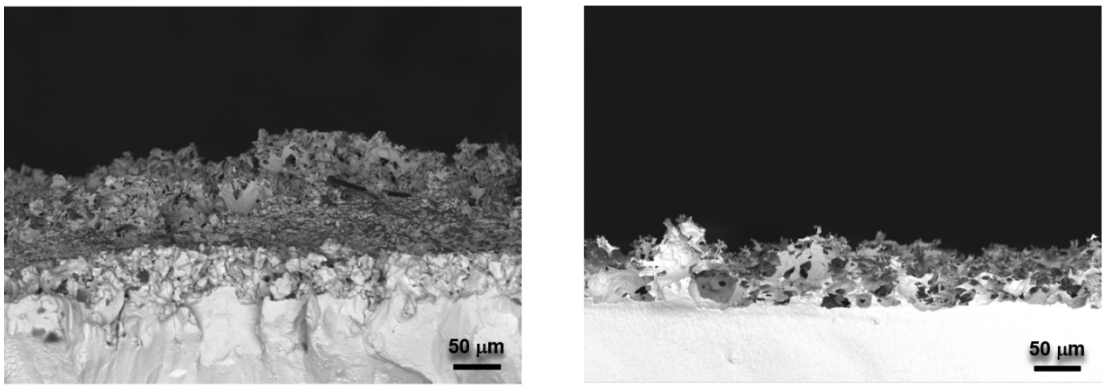

Fig. S2 The scanning electron microscope (SEM) section image of NPMG.

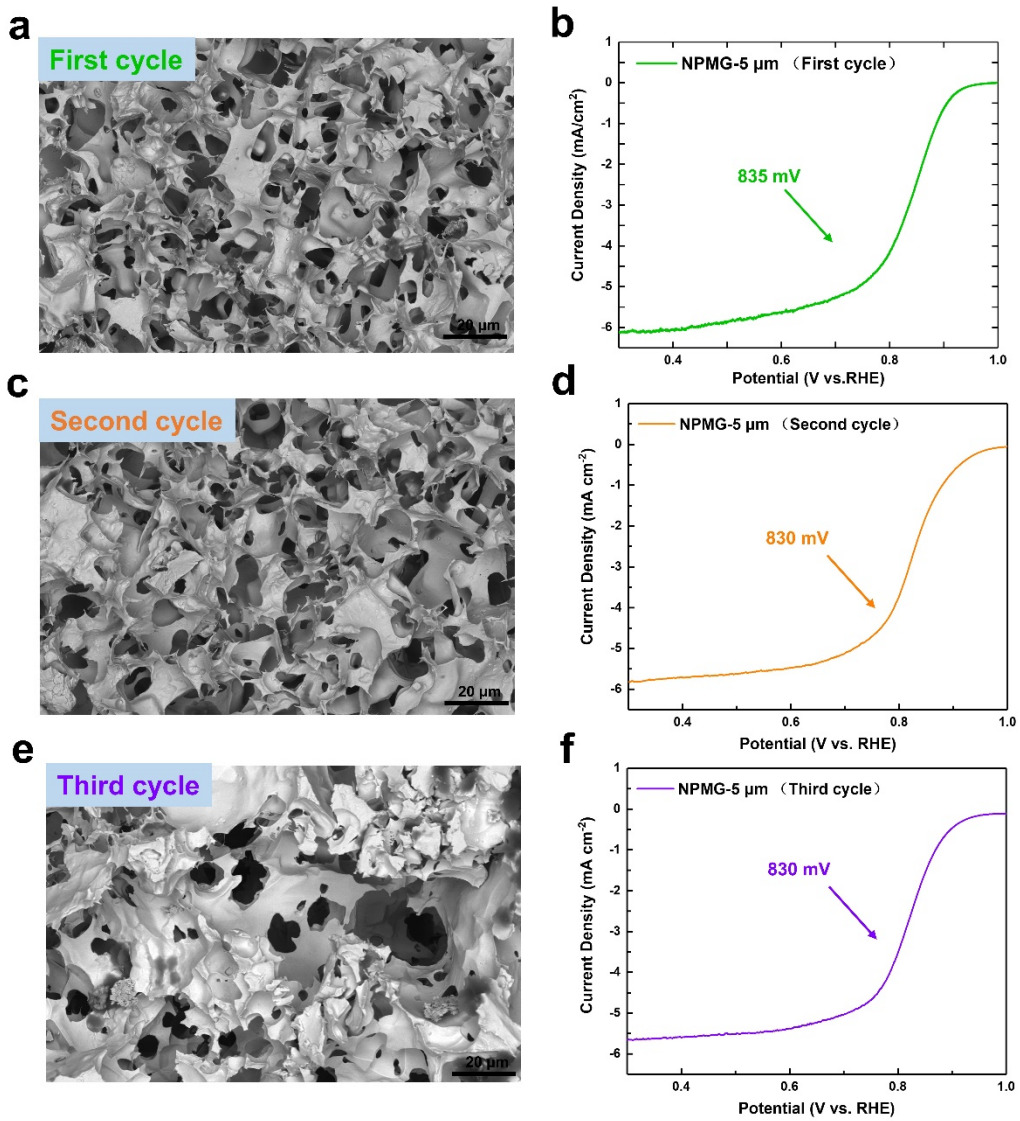

Fig. S3 (a) The surface morphology of NPMGs fabricated in the first cycle; (b) The half-wave potential of NPMGs fabricated in the first cycle; (c) The surface morphology of NPMGs fabricated in the second cycle; (d) The half-wave potential of NPMGs fabricated in the second cycle; (e) The surface morphology of NPMGs fabricated in the third cycle; (f) The half-wave potential of NPMGs fabricated in the third cycle.

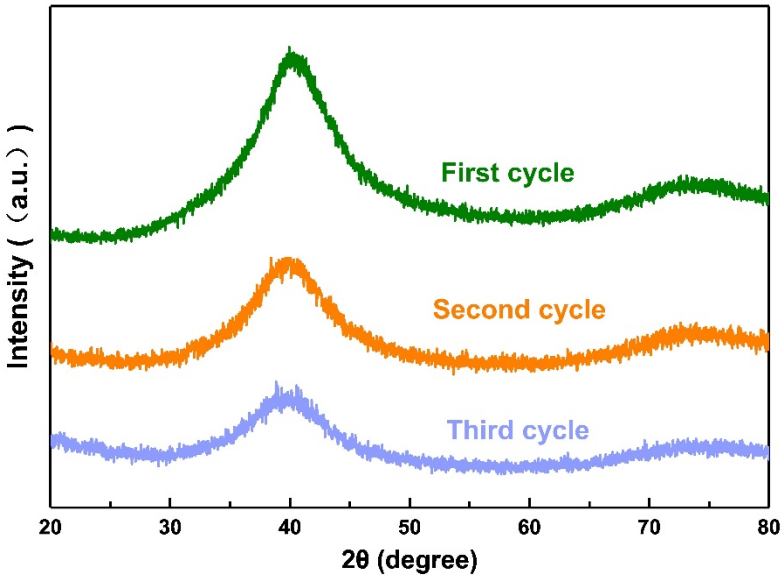

Fig. S4 The XRD pattern of original MG and reconstructed NPMGs.

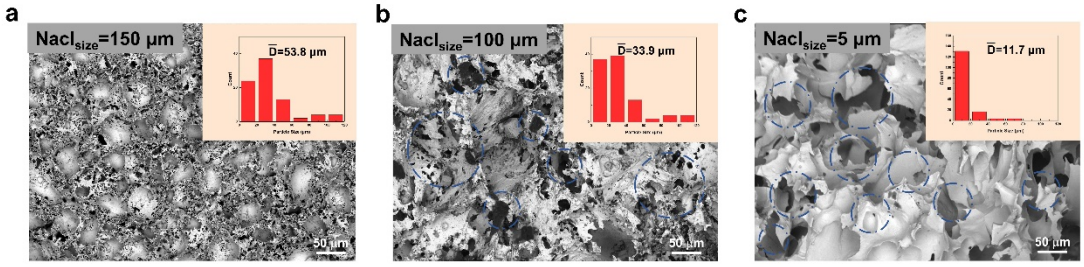

Fig. S5 The SEM of average pore size matched the size of the salt particles.

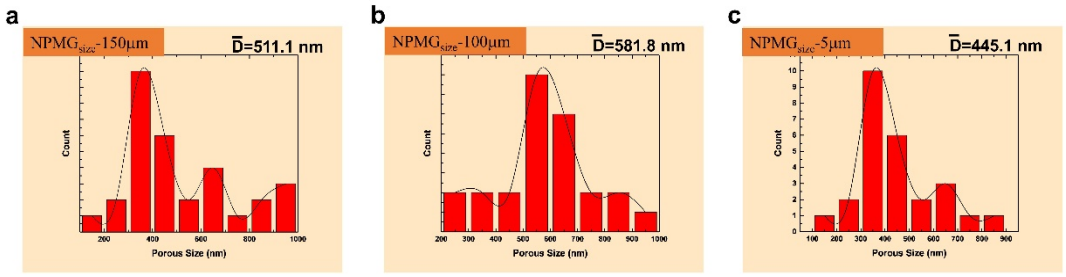

Fig. S6 The SEM of average nanopore size of NPMG-150μm, NPMG-100μm and NPMG-5μm.

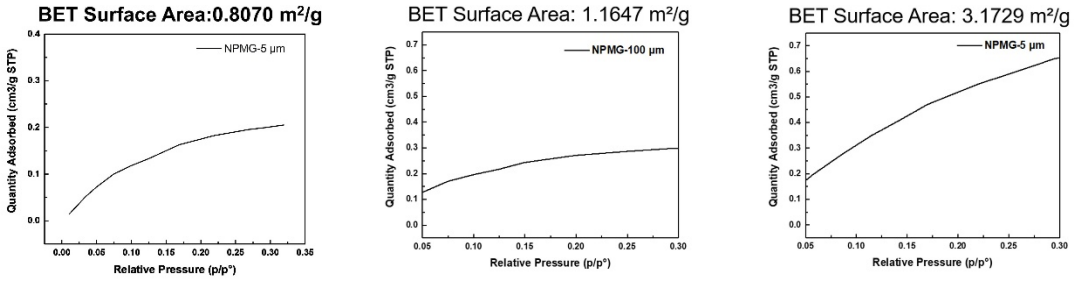

Fig. S7 Nitrogen adsorption curves (BET) for NPMG-150 µm, NPMG-100 µm and NPMG-5 µm samples.

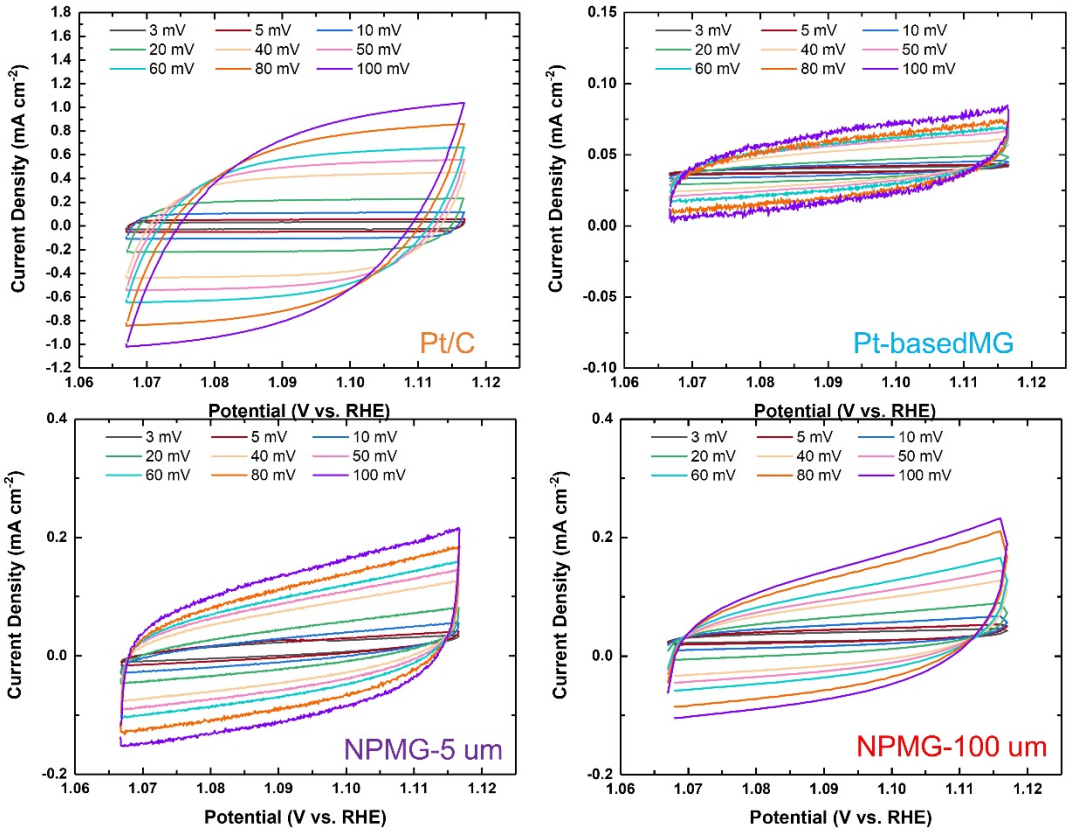

Fig. S8 (a) CV curves in 0.1 M KOH solution showing the double layer capacitance without electrochemcial reactions (a-c). The difference in current density ($\Delta J = Ja\text{-}Jc$) at 0.05 V (vs. Ag/AgCl) plotted against scan rate and fitted to a linear regression for the estimation of capacitance.

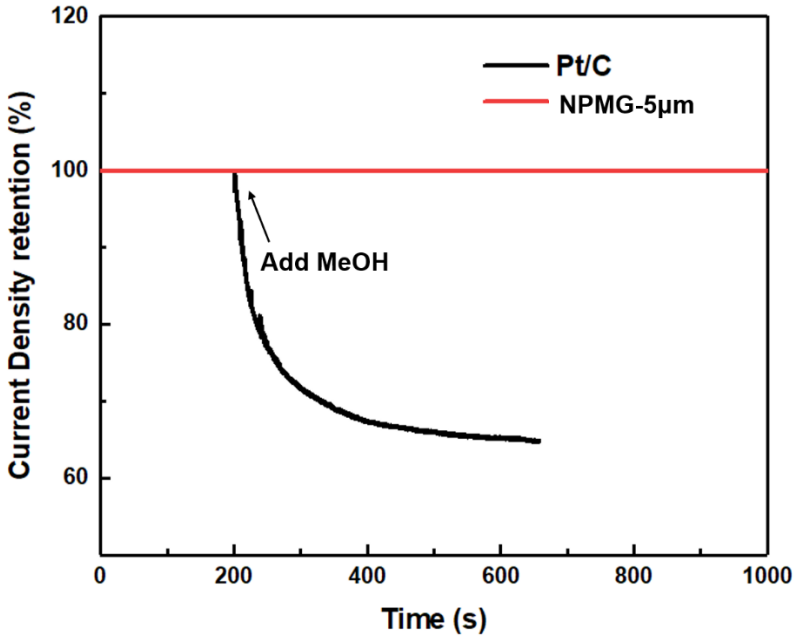

Fig. S9 (a) Chronoamperometric responses of NPMG and the benchmark Pt/C at 0.8 V in O_2-saturated 0.1 M KOH before and after addition of 2 M methanol under1600 rpm.

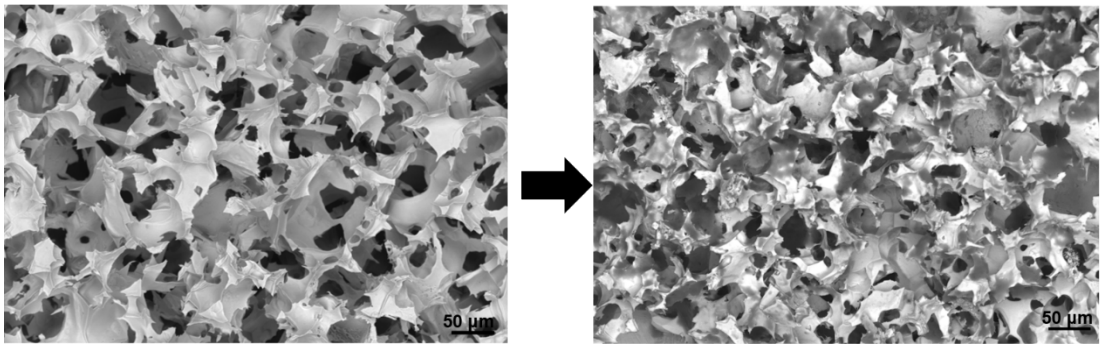

Fig. S10 the SEM analysis is performed to detect the surface structure of the sample after a long-time stability test.

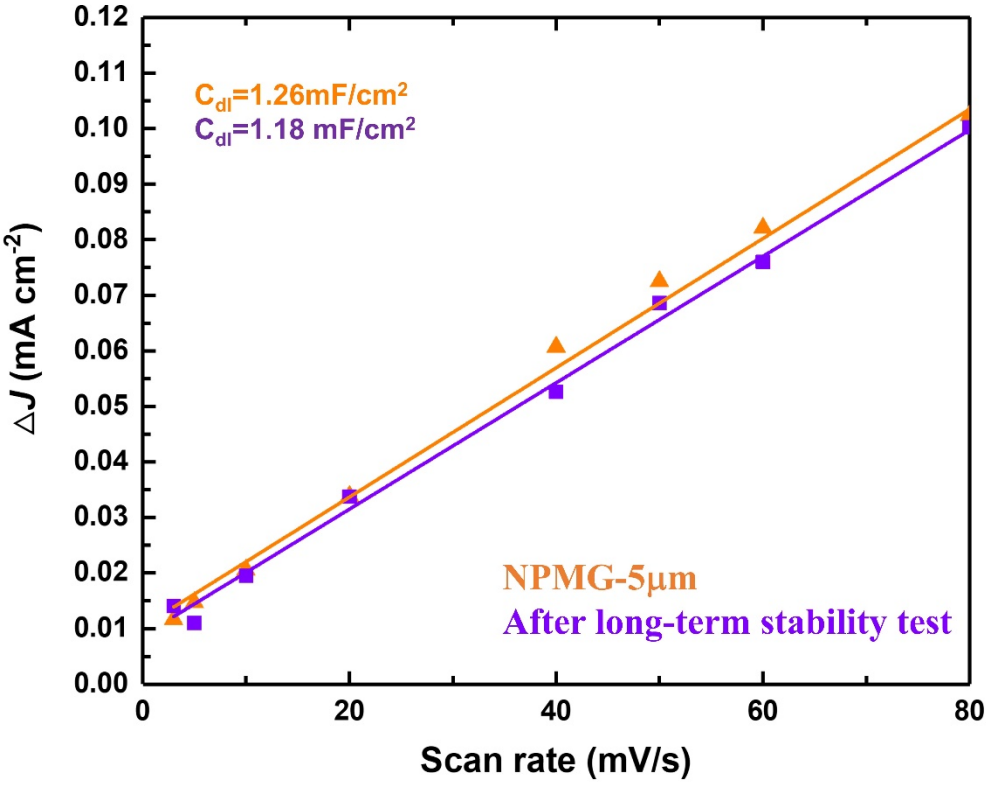

Fig. S11 Comparison of ECSA of samples before and after a long-time stability test.

Table S1. Comparison of Half-peak potential, Tafel slope and Stability for the ORR materials.

Catalysts	Half-peak potential mV vs. RHE	Tafel slope ($mVdec^{-1}$)	Stability (%)	Electrolyte	References
NPMG-5 μm.	835	54	100	0.1 M KOH	This
NPMG-100 μm	726	67	/	0.1 M KOH	work
20% Pt/C	823	72	75	0.1 M KOH	
CoFe-N-C	897	67.7	88	0.1 M KOH	[1]
FeCo-N-HCN	860	52.1	90	0.1 M KOH	[2]
CoFe/N-GCT	790	76	75	0.1 M KOH	[3]
A-FeCo@NCNs	870	80	84	0.1 M KOH	[4]
CoFePPy	840	81.8	81	0.1 M KOH	[5]
CoFe-NC	940	68	75	0.1 M KOH	[6]
CoFe/SN-C	843	98	46.1	0.1 M KOH	[7]
NiFe-NC	850	140	86.3	0.1 M KOH	[8]
NPSC-Co_2Fe1	850		70.9	0.1 M KOH	[9]
CoNi-SAs/NC	760	58.7	80	0.1 M KOH	[10]
Fe, Mn-N/C900	904	35	93	0.1 M KOH	[11]
FeCo-N-rGO	850	70	60	0.1 M KOH	[12]
(Fe,Co)@NGC	850	78	91	0.1 M KOH	[13]
Ni-N_4/GHSs/Fe-N_4	830	55	68.6	0.1 M KOH	[14]
NCAG/FeCo	890	64	89	0.1 M KOH	[15]
Pt/$CaMnO_3$	950	65	84	0.1 M KOH	[16]
Co_3O_4/rGO	890	101	37	0.1 M KOH	[17]
Co_3O_4/N/C	920	/	28	0.1 M KOH	[18]
Co@Co_3O_4/NCNT	820	83	31	0.1 M KOH	[19]
Fe_3O_4/N/C	920	/	25	0.1 M KOH	[20]
Fe-N-DSC	840	/	78	0.1 M KOH	[21]
FeCo@N-GCNT-FD	880	/	43	0.1 M KOH	[22]
Co@h-ZIF	906	128	/	0.1 M KOH	[23]
PtCu nanoparticles	915	87	21	0.1M$HClO_4$	[24]
Tin Selenide (SnSe)	750	137.5	/	0.1 M KOH	[25]
Co_3W_3C/NPG	790	/	/	0.1M$HClO_4$0	[26]
DS-Pd NPs	892	/	/	.1 M KOH	[27]
Co-N-C-MT/EA	810	77	13	0.1 M KOH	[28]
Fe-N-GO-400	820	60	85	0.1 M KOH	[29]
Fe-SA/HPC	910	68.7	/	0.1 M KOH	[30]
ZrO_2/NC	815	/	/	0.1 M KOH	[31]
WS_2/AC	860	68	96.4	N_2-aturated	[32]
WS_2/rGO	820	71	95.6	0.1 M KOH	[32]

Table S2. XPS element binding energy peak.

Sample	Before *J*-t	After *J*-t
BE（eV）		
Pt4f7 Scan A (Pt^0)	71.38	71.61
Pt4f5 Scan A (Pt^0)	74.58	74.20
Pt4f7 Scan B (Pt^{2+})	72.68	72.61
Pt4f5 Scan B (Pt^{2+})	76.08	76.00
Pt4f7 Scan C (Pt^{4+})	/	74.90
Pt4f5 Scan C (Pt^{4+})	/	77.80

Table S3. XPS Cu element binding energy peak

Sample	Before *J*-t	After *J*-t
BE（eV）		
Cu2p Scan A (Cu^0)	951.68	/
Cu2p Scan A (Cu^0)	932.08	/
Cu2p Scan B (Cu^{2+})	953.62	951.78
Cu2p Scan B (Cu^{2+})	933.88	933.08

Reference：

1. X. Zhou, J. Gao, Y. Hu, Z. Jin, K. Hu, K. M. Reddy, Q. Yuan, X. Lin and H. J. Qiu, *Nano Lett*, 2022, **22**, 3392-3399.
2. H. Li, Y. Wen, M. Jiang, Y. Yao, H. Zhou, Z. Huang, J. Li, S. Jiao, Y. Kuang and S. Luo, *Adv. Funct. Mater.*, 2021, **31**, 2011289.
3. X. Liu, L. Wang, P. Yu, C. Tian, F. Sun, J. Ma, W. Li and H. Fu, *Angew. Chem.*, 2018, **130**, 16398-16402.
4. Y. Luo, J. Zhang, J. W. Chen, Y. H. Chen, C. Y. Zhang, Y. J. Luo, G. Wang and R. L. Wang, *J. Catal.*, 2021, **397**, 223-232.
5. P. Li, Z. Jin, Y. Qian, Z. Fang, D. Xiao and G. Yu, *ACS Energy Lett.*, 2019, **4**, 1793-1802.
6. K. Wang, J. Liu, Z. Tang, L. Li, Z. Wang, M. Zubair, F. Ciucci, L. Thomsen, J. Wright and N. M. Bedford, *J. Mater. Chem. A*, 2021, **9**, 13044-13055.
7. C. Li, E. Zhou, Z. Yu, H. Liu and M. Xiong, *Appl. Catal., B*, 2020, **269**, 118771.
8. M. Ma, A. Kumar, D. Wang, Y. Wang, Y. Jia, Y. Zhang, G. Zhang, Z. Yan and X. Sun, *Appl. Catal., B*, 2020, **274**, 119091.
9. K. He, J. Zai, X. Liu, Y. Zhu, A. Iqbal, T. Tadesse Tsega, Y. Zhang, N. Ali and X. Qian, *Appl. Catal., B*, 2020, **265**, 118594.
10. X. P. Han, X. F. Ling, D. S. Yu, D. Y. Xie, L. L. Li, S. J. Peng, C. Zhong, N. Q. Zhao, Y. D. Deng and W. B. Hu, *Adv. Mater.*, 2019, **31**, 1905622.
11. S. P. Gong, C. L. Wang, P. Jiang, L. Hu, H. Lei and Q. W. Chen, *J. Mater. Chem. A*, 2018, **6**, 13254-13262.
12. X. Fu, Y. Liu, X. Cao, J. Jin, Q. Liu and J. Zhang, *Appl. Catal., B,* 2013, **130-131**, 143-151.
13. J. Xi, Y. Xia, Y. Xu, J. Xiao and S. Wang, *Chem. Commun.*, 2015, **51**, 10479-10482.
14. J. Chen, H. Li, C. Fan, Q. Meng, Y. Tang, X. Qiu, G. Fu and T. Ma, *Adv. Mater.*, 2020, **32**, 2003134.
15. Y. Chen, S. Hu, F. Nichols, F. Bridges, S. Kan, T. He, Y. Zhang and S. Chen, *J. Mater. Chem. A*, 2020, **8**, 11649-11655.
16. X. P. Han, F. Y. Cheng, T. R. Zhang, J. G. Yang, Y. X. Hu and J. Chen, *Adv. Mater.*, 2014, **26**, 2047-2051.
17. J. Xiao, Q. Kuang, S. Yang, F. Xiao, S. Wang and L. Guo, *Sci. Rep.*, 2013, **3**, 1-8.
18. G. Zhang, C. Li, J. Liu, L. Zhou, R. Liu, X. Han, H. Huang, H. Hu, Y. Liu and Z. Kang, *J. Mater. Chem. A*, 2014, **2**, 8184-8189.
19. J. Xiao, C. Chen, J. Xi, Y. Xu, F. Xiao, S. Wang and S. N. Yang, *Nanoscale*, 2015, **7**, 7056-7064.
20. Y. Su, H. Jiang, Y. Zhu, X. Yang, J. Shen, W. Zou, J. Chen and C. Li, *J. Mater. Chem. A*, 2014, **2**, 7281-7287.
21. Z. Huang, H. Pan, W. Yang, H. Zhou, N. Gao, C. Fu, S. Li, H. Li and Y. Kuang, *ACS nano*, 2018, **12**, 208-216.
22. L. An, N. Jiang, B. Li, S. Hua, Y. Fu, J. Liu, W. Hao, D. Xia and Z. Sun, *J. Mater. Chem. A*, 2018, **6**, 5962-5970.
23. X. Liu, W. Zhang, X.-H. Liu, K. Li and X. Zhang, *J. Electroanal. Chem.*, 2022, **906**, 116023.
24. S. Di, W. Liu, C. Guo, F. Wang, A. Bulanova, A. Mebel and H. Zhu, *J. Power Sources*, 2022, **533**, 231270.
25. Z. Feng, C. D. Jadhav, G. P. Patil, Y. Wang, C. Zhang, V. S. Baviskar, Z. Jia and R. Minnes, *J.*

Electroanal. Chem., 2022, **916**, 116381.
26. B. Li, J. Zhou, L. Zhang and Z. Li, *RSC Adv.*, 2018, **8**, 12292-12299.
27. M. Ma, Y. Zhang, Y. Ji, Q. Shao, K. Yin, W. Zhu, J. Yang, F. Liao, Z. Fan, Y. Liu, Y. Li, M. Shao and Z. Kang, *Appl. Catal., B*, 2022, **315**, 121549.
28. D. Xili, Q. Zhou and L. Zhang, *J. Alloys Compd.*, 2022, **911**, 165072.
29. R. Zhao, J. Xia, P. Adamaquaye and G. l. Zhao, *ChemistrySelect*, 2022, **7**, e202200616.
30. S. Wu, H. Liu, G. Lei, H. He, J. Wu, G. Zhang, F. Zhang, W. Peng, X. Fan and Y. Li, *Chem. Eng. J.*, 2022, **441**, 135849.
31. M. Wang, H. Zheng, Y. Dong, Z. Jin, S. Liao, W. Gong, X. Li, Z. Li, M. Xia and J. Wang, *Appl. Phys. Lett.*, 2022, **120**, 261903.
32. J. Tang, C. Wang, H. Zhang and J. Guo, *J. Alloys Compd.*, 2022, **911**, 164991.